Exploring the impact of digestive physicochemical parameters of adults and infants on the pathophysiology of Cryptosporidium parvum using the dynamic TIM-1 gastrointestinal model

Julie Tottey, Lucie Etienne-Mesmin, Sandrine Chalançon, Alix Sausset, Sylvain Denis, Carine Mazal, Christelle Blavignac, Guillaume Sallé, Fabrice Laurent, Stéphanie Blanquet-Diot, et al.

TITLE

Exploring the impact of digestive physicochemical parameters of adults and infants on the pathophysiology of *Cryptosporidium parvum* using the dynamic TIM-1 gastrointestinal model

AUTHORS

Julie Tottey[1], Lucie Etienne-Mesmin[2], Sandrine Chalançon[2], Alix Sausset[1], Sylvain Denis[2], Carine Mazal[2], Christelle Blavignac[3], Guillaume Sallé[1], Fabrice Laurent[1], Stéphanie Blanquet-Diot[2], Sonia Lacroix-Lamandé[1]

[1]UMR 1282 ISP, Infectiologie et Santé Publique, INRAE, Université de Tours, Nouzilly, France; [2]UMR 454 MEDIS, Microbiologie Environnement Digestif et Santé, Université Clermont Auvergne, INRAE, Clermont-Ferrand, France; [3]Centre Imagerie Cellulaire Santé, Université Clermont Auvergne, Clermont-Ferrand, France.

Corresponding author: Julie Tottey

ABSTRACT

Background

Human cryptosporidiosis is distributed worldwide, and it is recognised as a leading cause of acute diarrhoea and death in infants in low- and middle-income countries. Besides immune status, the higher incidence and severity of this gastrointestinal disease in young children could also be attributed to the digestive environment. For instance, human gastrointestinal physiology undergoes significant changes with age, however the role this variability plays in *Cryptosporidium parvum* pathogenesis is not known. In this study, we analysed for the first time the impact of digestive physicochemical

parameters on *C. parvum* infection in a human and age-dependent context using a dynamic *in vitro* gastrointestinal model.

Results

Our results showed that the parasite excystation, releasing sporozoites from oocysts, occurs in the duodenum compartment after one hour of digestion in both child (from 6 months to 2 years) and adult experimental conditions. In the child small intestine, slightly less sporozoites were released from excystation compared to adult, however they exhibited a higher luciferase activity, suggesting a better physiological state. Sporozoites collected from the child jejunum compartment also showed a higher ability to invade human intestinal epithelial cells compared to the adult condition. Global analysis of the parasite transcriptome through RNA-sequencing demonstrated a more pronounced modulation in ileal effluents compared to gastric ones, albeit showing less susceptibility to age-related digestive condition. Further analysis of gene expression and enriched pathways showed that oocysts are highly active in protein synthesis in the stomach compartment, whereas sporozoites released in the ileum showed downregulation of glycolysis as well as strong modulation of genes potentially related to gliding motility and secreted effectors.

Conclusions

Digestion in a sophisticated *in vitro* gastrointestinal model revealed that invasive sporozoite stages are released in the small intestine, and are highly abundant and active in the ileum compartment, supporting reported *C. parvum* tissue tropism. Our comparative analysis suggests that physicochemical parameters encountered in the child digestive environment can influence the amount, physiological state and possibly invasiveness of sporozoites released in the small intestine, thus potentially contributing to the higher susceptibility of young individuals to cryptosporidiosis.

KEYWORDS

Cryptosporidium; Apicomplexa; *in vitro* digestive model; physicochemical parameters; child and adult digestion

BACKGROUND

The zoonotic disease cryptosporidiosis caused by the protozoan Apicomplexa parasite *Cryptosporidium* is endemic in many low-income countries and potentially epidemic in high-income countries. This enteric disease leads to watery diarrhoea that can be life-threatening in individuals with an immature or a compromised immune system. Results from cohort studies have consistently shown that young age is associated with a higher risk of *Cryptosporidium* infection (1). Accordingly, *Cryptosporidium* infection is particularly associated with prolonged (7–14 days) or even persistent (≥ 14 days) diarrhoea during childhood, and can also lead to malnutrition and growth deficiency (1). Cryptosporidiosis is considered as one of the most common causes of infectious moderate-to-severe diarrhoea in children under the age of two (2,3) and an important contributor to early childhood mortality in low-resource settings (4), thus constituting a serious public health concern. In 2016, acute infections due to *Cryptosporidium* caused more than 48000 deaths in children under 5 years and more than 4.2 million disability-adjusted life-years lost (5).

Cryptosporidium parvum is one of the two most relevant *Cryptosporidium* species to humans and is transmitted primarily by the fecal–oral route either by direct contact with an infected human or animal or indirectly via food or water contaminated by oocysts (6). Once ingested, *C. parvum* oocysts excyst in the gastrointestinal tract, releasing infective and motile sporozoites that invade intestinal epithelial cells. The parasite life cycle then progresses through three rounds of asexual replication (7) before shifting to sexual reproduction and then to the production of a high number of infectious oocysts that ensure either auto-infection of the same host by infecting nearby intestinal cells or transmission in the environment after release in the faeces.

The higher incidence and severity of cryptosporidiosis reported in children under the age of two can be first attributed to their immature immune status, making them as susceptible to the infection by the parasite as immunocompromised adults (8). Nevertheless, other factors, such as those associated with the digestive environment (*i.e.,* immaturity of digestive processes, intestinal epithelium and resident microbiota) where *C. parvum* infection takes place, could also contribute to the age-dependent nature of symptomatic cryptosporidiosis. Consequently, there is a crucial need to investigate *C. parvum* pathogenesis considering the gastrointestinal physiology that varies greatly with age (9), especially in light of the differences in digestive physicochemical parameters encountered in children, compared to adults.

Due to obvious ethical and technical reasons, it remains very difficult to evaluate the pathophysiology of food- or water-borne pathogens in the human gastrointestinal tract, especially in pediatric populations. *In vitro* gastrointestinal models represent an appropriate alternative to *in vivo* assays to study the impact of digestive physicochemical parameters alone (*i.e.,* independently of any other influencing factors from the host) in a nutritional, pharmaceutical, toxicological or microbiological context. Among the available gastrointestinal systems, the computer-controlled TNO (Toegepast Natuurwetenschappelijk Onderzoek) gastroIntestinal Model-1 (TIM-1), which combines multi-compartmentalisation and dynamism, is one of the most complete *in vitro* simulators of the human upper gastrointestinal tract (10). By reproducing physiologically relevant conditions, the TIM-1 system allows the closest simulation of *in vivo* dynamic events occurring within the human stomach and three compartments of the small intestine. As a result, it has been successfully used for a diversity of applications in the past, for instance in an array of pathogen-related microbiological studies (10–16). As an example, the TIM-1 model has been used to demonstrate that the variability in human digestive physicochemical parameters that occurs between child and adult populations could play a role in *E. coli* O157:H7 pathogenesis, which is considerably more severe in children than in adults (12).

Within this framework, we designed an original approach to question for the first time the impact of digestive physicochemical parameters on *C. parvum* infection, in a human and age-dependent context.

The aim of the present study was to use the sophisticated TIM-1 model for a comparative analysis of *C. parvum* infection under the digestive conditions encountered in young children (from 6 months to 2 years) or in adults following the simulated digestion of a glass of contaminated water. Various parasite parameters, from the parasite excystation kinetics and global gene expression, to the sporozoite physiological state and infectivity, were monitored throughout the simulated human digestions.

METHODS

Cells and parasites

Human ileocecal adenocarcinoma cells (HCT-8) were purchased from the American Type Culture Collection, cultured in RPMI 1640 with phenol red supplemented with 2 mM GlutaMAX™, 10% (v/v) heat-inactivated fetal bovine serum (FBS), 1 mM sodium pyruvate, 50 U/ml penicillin, and 50 µg/ml streptomycin and maintained at 37°C in a humidified atmosphere under 5% CO_2. The *C. parvum* INRAE Nluc strain was generated by transgenesis to produce Nluc-expressing parasites, and purified as described in Swale *et al.*, 2019 (17).

In vitro digestions in the TIM-1 gastrointestinal model

The TIM-1 model (TNO, Zeist, The Netherlands) consists of four successive compartments simulating the human stomach and the three segments of the small intestine (duodenum, jejunum, and ileum) (Figure 1). The main parameters of digestion, such as body temperature, pH, peristaltic mixing and transport, gastric, biliary, and pancreatic secretions and passive absorption of small molecules and water, are reproduced as accurately as possible, as already described (16). The TIM-1 system was programmed to reproduce, based on *in vivo* data, the physicochemical digestive conditions observed in a healthy adult or a young child (from 6 months to 2 years) when a glass of water is ingested as previously described (12). The TIM-1 system was inoculated with a parasite suspension consisting of 200 mL of mineral water (Volvic®, Danone, France) experimentally contaminated with 1×10^8 oocysts of the *C. parvum* INRAE Nluc strain. Two sets of experiments were performed: gastric

118 digestions where the stomach compartment was solely used (total duration of 60 min) and
119 gastrointestinal digestions using the entire TIM-1 model (total duration of 300 min). Digestions were
120 run in triplicate.

121 **TIM-1 sampling**

122 Samples were taken in the initial parasite suspension (t=0) and regularly collected during *in vitro*
123 digestions from each digestive compartment (stomach, duodenum, jejunum, and ileum) to evaluate
124 parasite excystation kinetics, sporozoite luciferase activity and host cell invasion (Figure 1). Gastric
125 and ileal effluents were also collected on ice and pooled on 0-20, 20-45, and 45-60 min for gastric
126 digestions and hour-by-hour during 5 h for gastrointestinal digestions. Gastric and ileal effluents
127 collected during 0-20 min and 120-180 min, respectively, were used for RNA extraction.

128 **Parasite excystation kinetics**

129 The parasite excystation success was monitored in three independent experiments by flow cytometry
130 from samples collected regularly from each digestive compartment during *in vitro* digestions in the
131 TIM-1 system. Prior to each TIM-1 digestion assay, flow cytometry controls and gating strategy on
132 forward-angle light scatter/side-angle light scatter were performed based on analysis of intact (non-
133 excysted) oocysts, and non-filtered or 5 µm-filtered (Sartorius AG, Göttingen, Germany) *in vitro*
134 excysted parasites (Figure 2.A). Such controls aimed to differentiate *C. parvum* oocysts from
135 sporozoites and from the background. Flow cytometry analyses were all performed immediately after
136 sample collection on a BD™ LSR II cytometer and data were collected with the BD FACSDiva™
137 Software version 9 (BD Biosciences, Franklin Lakes, USA). Results are expressed as relative
138 percentages of parasites detected as intact oocyst stages in each digestive compartment compared to
139 the corresponding age condition's inoculum.

140 **Sporozoite luciferase activity**

141 The physiological state of *C. parvum* sporozoites was monitored in three independent experiments for
142 the initial parasite suspension and for samples collected regularly from the duodenum, jejunum and

ileum compartments during *in vitro* digestions in the TIM-1 system. Immediately after collection, each sample was washed with phosphate-buffered saline (PBS), filtered through a 5 µm membrane (Sartorius AG, Göttingen, Germany) to discard oocysts and empty shells, centrifuged (10000 ×g, 3 min, 4°C) and resuspended in PBS. The luciferase activity expressed by the recovered sporozoites was assessed (three replicates for each sample) using the Nano-Glo® Luciferase Assay System (Promega Corporation, Madison, USA). The sporozoites were mixed (v/v) with the Nano-Glo® Luciferase Assay Buffer containing 1:50 of the Nano-Glo® Luciferase Assay Substrate and the luminescence was measured with the GloMax®-Multi Detection System (Promega Corporation, Madison, USA). The luciferase activity expressed by sporozoites collected from the TIM-1 compartments was normalised to the initial parasite suspension for each assay.

Parasite invasion assay

The ability of *C. parvum* sporozoites to invade intestinal epithelial cells was monitored in two independent experiments for samples collected regularly from the small intestinal compartments during *in vitro* digestions. Immediately after collection, each parasite sample was washed with sterile PBS, filtered through a 5 µm membrane (Sartorius AG, Göttingen, Germany) to discard oocysts and empty shells, centrifuged (10000 ×g, 3 min, 4°C) and resuspended into sterile PBS. The recovered sporozoites were immediately used to infect HCT-8 cell monolayers grown to 80% confluence in Nunc™ F96 MicroWell™ white polystyrene plates (Thermo Fisher Scientific, Waltham, USA). After 2.5 hours, cells were washed twice with sterile PBS and used to analyse the invasion of parasites (six replicates per sample). The luciferase activity was detected directly from the infected cell monolayers using the Nano-Glo® Luciferase Assay System (Promega Corporation, Madison, USA) and the GloMax®-Multi Detection System as described above. Luciferase activity data were normalised to the luminescence background detected in uninfected cultures.

Parasite RNA extraction

RNA samples were collected on ice from the initial parasite suspension and from gastric (0-20 min) or ileal (120-180 min) effluents during *in vitro* digestions. Samples were then centrifuged (10000 ×g, 5

min, 4°C), resuspended into 500 µL TRI Reagent® (Sigma-Aldrich, Saint-Louis, USA) and subjected to 5 cycles of [1 min vortexing - 1 min on ice] after addition of 0.5 mm glass beads. The lysates were centrifuged (10000 ×g, 10 min, 4°C) and the supernatants were mixed with absolute ethanol and transferred to a Zymo-Spin™ IC column (Direct-zol™ RNA Microprep kit, Zymo Research, Irvine, USA). Total RNAs were isolated according to the manufacturer's instructions. Any contaminating genomic DNA was removed using the DNase I Set kit (Zymo Research). RNA was further purified with the RNA Clean & Concentrator™-5 kit (Zymo Research) and concentrations measured using the Qubit™ 2.0 fluorometer using RNA HS assay kit (Thermo Fisher Scientific). RNA quality was assessed using the Agilent 2100 Bioanalyzer system and the RNA 6000 Pico kit (Agilent Technologies, Santa Clara, USA).

RNA-Seq analysis of differentially expressed genes

Library construction and sequencing were performed by Helixio (Biopôle Clermont-Limagne, Saint-Beauzire, France). The RNA library preparation was performed using the QuantSeq 3′ mRNA-Seq Library Prep Kit FWD for Illumina (Lexogen, Vienna, Austria). A total of 15 RNA-Seq libraries were generated, corresponding to 3 libraries for each experimental group, and then sequenced with the NextSeq® 500 System (Illumina, San Diego, USA) using a single-read sequencing of 76 bp length configuration. Raw sequence data were assessed for quality using the FastQC v0.11.3 tool (Babraham Institute, Cambridge, UK). Sequenced reads were aligned to the *C. parvum* IOWA-ATCC reference genome (genome assembly ID: ASM1524537v1) using the STAR software (18). The number of sequences reads that mapped the *C. parvum* genome varied between 11 and 14 million per library. Gene counts were determined using the STAR software. The R–based packages DESeq2 (19) and edgeR (20) were used to normalise data, perform descriptive analysis as well as all pairwise comparisons to determine the differentially expressed genes between experimental groups. Clustering of transcriptomic profiles was assessed through a principal-component analysis (PCA) using normalised RNA-Seq data of a set of 2430 filtered genes, for which at least 10 reads were counted in a minimum of three samples. The *P*-values generated during pairwise comparisons were adjusted for multiple testing with the Benjamini-Hochberg procedure which controls for false discovery rate

(FDR). Genes were considered to be differentially expressed between two experimental groups at an FDR adjusted *P*-value < 0.05. Gene Ontology (GO) (21,22) and KEGG Metabolic Pathway (23–25) enrichment analyses were performed on differentially expressed genes on CryptoDB (26).

Statistical analysis

Graphs and boxplots were generated using GraphPad Prism version 10.2.3 and statistical analyses were performed using R version 4.3.1. Significant differences in luciferase activity and invasion ability data according to time of digestion were tested using a nonparametric analysis of longitudinal data with the R package "nparLD" (27) version 2.2. In case of a significant time effect, pairwise comparisons between time points were calculated with the R package "nparcomp" (28) version 3.0. $P < 0.05$ was considered statistically significant and indicated by non-corresponding letters (lowercase for the child condition and capitals for the adult condition). The Mann-Whitney non-parametric test was performed to test the effect of treatment (child *vs.* adult) for each time point and to analyse luciferase data collected from live or heat-killed parasites (Additional file 1), with significant differences indicated as follows: * $P < 0.05$; ** $P < 0.01$; *** $P < 0.001$; **** $P < 0.0001$.

RESULTS

Parasite excystation kinetics in the simulated upper gastrointestinal tract

To establish the gating strategy, flow cytometry controls were performed during *in vitro* excystation of parasites (Figure 2.A). These controls showed that intact oocysts were abundant before excystation and easily discriminated from empty shells and sporozoites during the process of excystation (when non-filtered). In contrast, intact oocysts were scarcely detected in filtered excysted samples, in which mostly sporozoites could be observed.

The same gating strategy was then used to monitor parasite excystation kinetics during child and adult digestions in the TIM-1 system. Time of digestion had an overall significant effect on parasite excystation in both child ($P < 0.0001$) and adult ($P < 0.0001$) conditions. In the simulated stomach

compartment, the proportion of intact oocysts (*i.e.*, non-excysted parasites) remained high regardless of the age condition, with 80.4 ± 7.2% and 81.4 ± 10.1% intact oocysts detected at 45 min for child and adult digestion, respectively (Figure 2.B, Table 1). In contrast, subsequent transit in the duodenal compartment marked a brutal decrease in the proportion of intact oocysts detected, which dropped to 4.5 ± 0.3% and 1.5 ± 0.3% at 60 min for child and adult condition, respectively. The parasite excystation further progressed in the small intestine compartments and reached a minimal amount of intact oocysts detected for both conditions in the ileal compartment by the end of digestion (1.0 ± 0.1% and 0.6 ± 0.1% at 300 min for the child and the adult digestion, respectively). The quantity of intact oocysts detected in the child's small intestine was consistently higher when compared to the adult condition whatever the compartment and time considered (Table 1). Our results suggest that sporozoites released from excystation in the small intestine would be slightly less abundant in infants compared to adults.

Table 1. Percentage of parasites detected as intact oocysts for the child or adult TIM-1 experiments.

Age condition	TIM-1 digestion	0 min Ino	20 min Sto	45 min Stomach	60 min Duo	120 min Jej	180 min Ile	300 min Ile
CHILD	1	100	98.2	93.5	3.8	1.9	1.8	1.1
	2	100	73.5	68.6	4.7	2.6	2.4	0.9
	3	100	86.8	79.0	5.0	2.7	2.6	1.0
ADULT	1	100	101.5	99.5	1.4	1.3	1.2	0.9
	2	100	83.2	64.7	2.0	1.4	1.1	0.6
	3	100	90.1	79.9	1.0	0.7	0.6	0.4

The parasite excystation kinetics was analysed by flow cytometry during child or adult digestion in the TIM-1 system. Samples recovered from the inoculum (Ino) or from the stomach (Sto), duodenum (Duo), jejunum (Jej) or ileum (Ile) compartments were immediately processed after collection. Values from three independent child or adult digestion in the TIM-1 system are expressed as relative percentages of intact oocysts as compared with that of the inoculum for each digestion assay.

Physiological state and invasion ability of *C. parvum* sporozoites collected from the *in vitro* small intestine

The physiological state of the sporozoites released following excystation in the small intestine of the TIM-1 system was estimated through analysis of the activity of the luciferase reporter gene that is

constitutively expressed by the parasite strain (Figure 3.A). Time of digestion had an overall significant effect on sporozoite luciferase activity in both child ($P < 0.0001$) and adult ($P < 0.0001$) conditions. In the child small intestine, sporozoite relative luciferase activity significantly increased from 38.9 ± 12.1 normalised relative light units (RLUs) in the duodenum at 60 min and 950.5 ± 12.1 RLUs in the jejunum at 120 min to a maximum reached at 180 min in the ileum (2.0×10^4 ± 4.2×10^3 RLUs; $P < 0.0001$ between 60 min and 180 min and between 120 min and 180 min). During the last two hours of digestion, the relative luciferase activity detected in the child ileal compartment decreased (7.9×10^3 ± 1.4×10^3 RLUs) but remained significantly higher than the one detected in the duodenum and jejunum at the beginning of digestion ($P < 0.0001$ between 60 min and 300 min and between 120 min and 300 min). The luciferase activity kinetics of sporozoites collected from the adult digestions followed the same trend but at a much lower intensity, with a maximum reached of 706.7 ± 80.0 RLUs at 180 min in the ileum. Additionally, the relative luciferase activity expressed by sporozoites was consistently and significantly higher for the child condition when compared to the adult one, whatever the compartments of the small intestine and the time points ($P < 0.0001$ at 60, 120, 180 and 300 min). Controls performed on the *C. parvum* INRAE Nluc strain showed that the luciferase activity measured from excysted parasites was dependent on the quantity ($P < 0.01$ between 1×10^7 and 1×10^8 excysted parasites) and viability ($P < 0.01$ between live and heat-killed parasites) of parasites present in the sample (Additional file 1). In the TIM-1 small intestine under child condition, fewer sporozoites (Figure 2.B, Table 1) but a significantly higher luciferase activity (Figure 3.A) was detected compared to the adult condition.

The invasion ability of Nluc-expressing sporozoites collected and purified from the TIM-1 small intestine was assessed by *in vitro* infection of HCT-8 cell monolayers and subsequent determination of luciferase activity (Figure 3.B). Time of digestion had an overall significant effect on sporozoite ability to invade host cells in both child ($P < 0.0001$) and adult ($P < 0.0001$) conditions. The invasion of HCT-8 monolayers was observed to be low and stable for sporozoites collected from the duodenum at 60 min or from the jejunum at 120 min of both child (9.3×10^2 ± 3.4×10^2 RLUs and 1.4×10^3 ± 2.5×10^2 RLUs, respectively) and adult (3.0×10^2 ± 1.2×10^2 RLUs and

269 4.6□×□10^2 ± 1.6□×□10^2 RLUs, respectively) digestive conditions. The invasion ability was observed
270 to be significantly increased for sporozoites collected at 180 min from the child ileum (8.0□×□10^3 ±
271 3.0□×□10^3 RLUs; $P < 0.01$ between 180 min and other time points) or the adult ileum (4.8□×□10^3 ±
272 8.0□×□10^2 RLUs; $P < 0.0001$ between 180 min and other time points). By the end of digestion,
273 parasite invasion dropped to a level comparable to the one observed at 60 min or 120 min, with a
274 relative luminescence of 1.0□×□10^3 ± 2.8□×□10^2 or 5.1□×□10^2 ± 1.3□×□10^2 RLUs detected for
275 monolayers infected with sporozoites collected at 300 min in the child or adult ileum, respectively.
276 The invasion ability of sporozoites was significantly higher in children compared with adults only at
277 120 min in the jejunum ($P < 0.01$).

278 **Parasite gene expression following child or adult digestion in the TIM-1 model**

279 The parasite transcriptome modifications induced by adult or child digestions in the TIM-1 were
280 determined by whole transcriptome sequencing (RNA-Seq) for gastric (0-20 min) and ileal (120-180
281 min) effluents, and also for the initial inoculum as control. A principal component analysis (PCA) was
282 performed to evaluate the samples' distribution according to their expression profiles. The first (31%)
283 and second (16%) components represented most of the differential expression pattern with a
284 cumulative proportion of 47% (Figure 4.A). This PCA analysis revealed a segregation between
285 samples collected at different time points and from different TIM-1 compartments. The PCA plot
286 showed that all six samples from the ileal effluents were grouped together, and that the three inoculum
287 samples and the six samples from the gastric effluents formed two other distinct groups (*i.e.*, clusters),
288 despite samples 'Inoculum_3' and 'Stomach_Adult2' being more distant from their respective
289 replicates. For each cluster corresponding to samples collected from gastric or ileal effluents, no
290 further segregation by age could be observed, suggesting that most of the variance is explained by
291 time and/or digestive compartment, rather than simulated age (*i.e.*, child *vs.* adult). Indeed, pairwise
292 comparisons resulted in no or only one gene (Gene ID CPATCC_0017110: unspecified product)
293 whose expression was significantly modified (*i.e.*, showing an adjusted *P*-value [FDR] < 0.05 and a
294 minimum 2-fold regulation [log2FC > 1]) between the two age conditions when effluent was collected
295 in the gastric or in the ileal compartment, respectively (Figure 4.B, Additional files 2 and 3). In

296 contrast, expression profiles were more affected by time and/or digestive compartment, with for
297 example 22 genes whose transcription levels were modified between gastric samples and inoculum for
298 both age conditions, and 83 or 99 genes between gastric and ileal samples for child or adult conditions,
299 respectively. Furthermore, the strongest modulation of the parasite transcriptome was observed
300 between ileal samples and inoculum, with 190 genes whose transcription levels were significantly
301 affected in the adult digestive condition and up to 208 genes in the child.

302 Most of the differentially expressed genes (DEGs) detected in samples collected from the stomach
303 between 0 and 20 min and compared to the inoculum were found upregulated: 18/22 or 20/22 for child
304 or adult, respectively, with 14 genes shared by both age conditions (Figure 4.C, Additional files 4 and
305 5). An analysis of enriched gene ontology (GO) performed on these overexpressed genes in the
306 stomach of the child condition found two significantly enriched GO terms related to cellular
307 components (Additional files 4 and 6.A): ribonucleoprotein complex (FDR = 0.026) and ribosome
308 (FDR = 0.026), both associated with the translation process. Approximately two thirds (*i.e.*, 67.4% or
309 63.6% for child and adult conditions, respectively) of the DEGs identified in ileal samples compared
310 to gastric samples were found downregulated (Figure 4.C, Additional files 7 and 8). Thirty-two
311 significantly downregulated genes are shared by child and adult conditions, among which a gene
312 encoding a myosin motor domain containing protein (Gene ID CPATCC_0009620) showed a 6-fold
313 decrease. One gene encoding an actin protein (Gene ID CPATCC_0025920) showed a 3.8-fold
314 decrease, but only in the child condition. Among downregulated genes, GO enrichment analysis
315 revealed a single significantly enriched GO term related to a molecular function in the adult condition:
316 protein tyrosine/serine/threonine phosphatase activity (FDR = 0.024). Six genes that were found
317 significantly upregulated in the child ileum compared to the child stomach encode putative secreted
318 proteins, of which two are part of the SKSR family (Gene IDs CPATCC_0030860 and
319 CPATCC_0035410) and one is an alpha/beta hydrolase (Gene ID CPATCC_0025460), the latter being
320 also significantly upregulated in the adult condition. The GO enrichment analysis found six
321 significantly enriched GO terms in the child (FDR < 0.05), all related to diverse cellular components
322 (*i.e.*, nuclear or organelle compartments) (Additional files 6.B and 7). The expression of a gene

encoding an actin family protein showed a 40-fold significant increase in the adult condition (Gene ID CPATCC_0036850).

As mentioned above, the strongest modification of the parasite transcriptome was observed for ileal samples between 120 and 180 min of digestion when compared to the initial inoculum (Figure 4.B, Additional files 9 and 10). For instance, 98 and 83 DEGs were significantly downregulated in child and adult ileum, respectively, with 56 genes shared by both age conditions (Figure 4.C). Among shared downregulated genes, the expression of the gene CPATCC_0009860 encoding the cryptosporidial mucin, also designated as glycoprotein-900 (GP900), was significantly decreased by a 4.8-fold. The myosin motor domain containing protein-encoding gene CPATCC_0009620 was also significantly downregulated in the ileum compared to the inoculum (9.7- or 6.8-fold decrease in the child or the adult condition, respectively). Subsequent metabolic pathway enrichment analysis interrogating the KEGG pathway database with significantly downregulated genes highlighted glycolysis/gluconeogenesis as the single significantly enriched pathway in the child ileum (FDR = 0.029) (Figure 5.A). The expression of 110 and 107 genes was significantly increased in child and adult ileum, respectively, among which the majority (*i.e.*, 81 genes) was shared by both age conditions (Figure 4.C). For example, four genes encoding putative secreted protein were significantly upregulated in both child and adult ileum, when compared to the inoculum. Among those genes, one relates to the putative secreted alpha/beta hydrolase previously identified (Gene ID CPATCC_0025460) and two belong to the SKSR gene family (CPATCC_0000030 and CPATCC_0030860). GO enrichment analysis performed on significantly upregulated genes highlighted 22 significantly enriched GO terms (FDR < 0.05) shared by child and adult (Figure 5, Additional files 9 and 10). Among these, the top three shared enriched GO terms were associated with cellular components and identified as intracellular structure, intracellular organelle and organelle. Gene expression was shared by both age conditions and associated to 26 or 32 genes out of the 110 (23.6%) or 107 (29.9%) significantly upregulated genes detected in the child or the adult condition, respectively. Using the KEGG pathway database, folate biosynthesis was identified as the top one enriched pathway in child (FDR = 0.0008) or adult (FDR = 0.010) ileum compared to the inoculum,

and was mostly associated with upregulated helicase-encoding genes. Interestingly, the expression of one gene associated to myosin complex and cytoskeletal motor activity (Gene ID CPATCC_0021030), was highly significantly upregulated by a 1978-fold in the child ileum, compared to the inoculum sample.

DISCUSSION

The goal of our study was to perform a comparative analysis of *C. parvum* infection under the digestive conditions encountered in young children (from 6 months to 2 years) *versus* those in adults. Due to the inherent limitations of *in vivo* experimentation within the host, the investigation of *C. parvum* excystation has only been performed to date with highly simplified *in vitro* approaches integrating only a few digestive parameters simultaneously (*e.g.*, temperature, pH) (29). Furthermore, these approaches have never been conducted under finely defined child *vs.* adult digestive conditions, nor combining digestive physicochemical properties with transit dynamism. Based on previous studies on other pathogens (10,12–14,16), we used the dynamic multicompartmental TIM-1 system as a suitable model to monitor *C. parvum* excystation along the simulated human upper gastrointestinal tract of both infant and adult conditions. Our study demonstrates for the first time that most oocysts are found intact in the simulated human stomach compartment 45 min after inoculation in the TIM-1 and that the excystation step occurs rapidly and is almost completed within the following 15 min and upon passage in the duodenal compartment. These data suggest that the majority of *C. parvum* oocysts do not undergo excystation until reaching the duodenum, thereby avoiding premature release and subsequent inactivation of the more susceptible sporozoite stages in the gastric acid environment. This is in accordance with the existence of two *Cryptosporidium* lineages that show adaptation to different excystation conditions, one displaying gastric tropism including parasite species that multiply in this gastric acidic environment (*e.g.*, *C. andersoni* and *C. muris*) and one exhibiting intestinal tropism (*e.g.*, *C. parvum* and *C. hominis*) (30). In order to maximise the delivery of sporozoites according to species tropism, excystation is thus activated by different host-derived triggers. In the TIM-1 system, mirroring *in vivo* situations, the excystation of *C. parvum* oocysts might have been triggered first by

376 elevation of the temperature to 37°C upon parasite inoculation into the system, followed by a drastic
377 change in pH upon passage from the acid gastric compartment to the alkaline duodenal one. Previous
378 *in vitro* studies investigating host-derived factors triggering *C. parvum* oocysts excystation have
379 reported that temperature increase and pH change play the most important roles in the transduction of
380 external signals across the oocyst wall to sporozoites (29,31–33). The digestive secretions (*i.e.*, bile
381 salts, trypsin and pancreatic juice) that the duodenal compartment receives in the TIM-1 system might
382 also play a role in *C. parvum* excystation process, although our knowledge of their precise role as
383 excystation triggers or putative synergistic effect is still limited. Interestingly, *in vitro* incubation of
384 oocysts in bile, in particular in sodium taurocholate following exposure to an acid pre-treatment, has
385 been shown to enhance parasite excystation, mimicking transition from the acidic gastric environment
386 to the alkaline small intestine (29,31,34).

387 Our flow cytometry analysis suggests that the excystation rate was slightly more efficient along the
388 simulated small intestine compartments upon adult digestive condition compared to the child one. This
389 could be attributable to specific differences in the physicochemical parameters described for child
390 *versus* adult physiology in a healthy state, which were subsequently implemented into the TIM-1
391 programs (12). For instance, the discrepancy in excystation success may be explained by the slower
392 and less pronounced gastric pH acidification in children (35,36) and/or by the lower concentrations of
393 various secretion components delivered in the child's duodenum, especially of bile salts (37,38)
394 known to enhance excystation (29,31,34).

395 The constitutively expressed luciferase marker was used as an indicator to assess sporozoite
396 physiological state, since the intensity of its robust and sensitive signal correlates directly with the
397 number and viability of parasites (Additional file 1). Taken together, our flow cytometry and
398 luciferase analyses suggest that the highest amount of released sporozoites is present in the simulated
399 ileum, and their physiological state peaks in this compartment at 180 min of digestion, regardless of
400 age conditions. This suggests that *C. parvum* has evolved an excystation process that ensures the
401 accumulation of the maximum number of freshly released sporozoites in the gastrointestinal segment
402 where this species shows the highest tissue tropism *in vivo*. While *C. parvum* has been reported to

colonise both proximal intestinal segments and the colon in different hosts (39,40), infections associated with this species are predominantly concentrated in the distal small intestine (41,42). For instance, recent *in vivo* bioluminescent imaging of a Nluc-expressing *C. parvum* strain throughout the intestinal tract of IFN-γ-KO mice clearly showed the parasites to be mainly localised in the ileum section as well as in the caecum (43).

Our results also suggest that simulated small intestine of the child condition is associated with fewer sporozoites on the one hand, but a significantly higher sporozoite luciferase activity on the other hand compared to the adult condition. Consequently, sporozoites residing in the intestinal tract of infants could be characterised by a higher viability or be in a less damaged state. In the context of a contamination by the major food- or waterborne pathogen enterohemorrhagic *Escherichia coli* (EHEC O157:H7 serotype), Roussel *et al.* used a similar TIM-1 setup to demonstrate that a higher amount of viable bacterial cells may reach the distal parts of the child's small intestine, compared to those of adults (12). These results might be attributed to less stringent conditions encountered by bacteria or *C. parvum* sporozoites in the child's intestinal tract, in regard to the two-fold lower concentration in bile salts and pancreatic secretions described for children compared to adults (37,38,44,45), also reproduced in the TIM-1 model. To our knowledge, the direct impact of various concentrations of duodenal secretions on *C. parvum* sporozoite survival has not yet been investigated. Therefore, we can not exclude that the significantly decreased physiological state observed for the sporozoites released in the adult small intestine may be the result of the detergent properties associated with higher concentrations of duodenal secretions encountered in this environment.

We then aimed to investigate whether the higher physiological state of *C. parvum* sporozoites observed in the child intestinal tract could also correlate with an increased infectivity. To this end, the TIM-1 system was combined for the first time with a cell culture assay, wherein we tested the capacity of sporozoites collected from the digestive compartments to invade human intestinal epithelial cells. The invasion assay suggests that sporozoites collected from the ileal compartment at 180 min of digestion have a significantly higher ability to invade HCT-8 cells, compared to other time points. This finding may reflect the slightly higher amount of sporozoites present in the ileum compartment,

as compared to the duodenum compartment for instance, but it may also be linked to the significantly higher sporozoites' physiological state and further emphases the tropism of *C. parvum* for the ileum *in vivo*. Interestingly, when collected from the same TIM-1 compartment, but at the end of the digestion process (300 min of digestion), sporozoites show a decreased luciferase activity and demonstrate a markedly reduced ability to invade host cells. In the literature, *C. parvum* sporozoites have been reported as somewhat fragile (46–48), surviving only for a few hours after release from the much more resilient oocyst stage. Our results are in agreement with this description and suggest that the infectivity potential of these vulnerable parasite stages may decrease drastically in the small intestine lumen if invasion of epithelial cells does not occur quickly after excystation. Our invasion assay shows that, although a lower amount of sporozoites was inoculated to host cells under the child condition (*i.e.,* according to our flow cytometry data), these sporozoites exhibit equivalent or even significantly higher invasion ability compared to the adult condition, most likely due to their "better" physiological state. Thus, our results suggest that age-related variability in digestive physicochemical parameters may modulate different features of sporozoite physiology, and therefore participate in higher susceptibility of young children to *C. parvum* infection compared to adults.

In this study, we also aimed to characterise the modulation of the *C. parvum* gene expression in response to the various digestive physicochemical parameters encountered by the parasite in two different compartments of the child or adult gastrointestinal tract. Intriguingly, our results revealed that the parasite transcriptome is almost exclusively affected by the time and/or compartment of digestion in the TIM-1, rather than by the simulated age (*i.e.*, child *vs.* adult). This observation suggests that parasite gene expression is predominantly governed by the succession of shifts in digestive environmental conditions and the duration of digestion, rather than by more subtle physicochemical specificities associated with age condition. In contrast, previous RT-qPCR analyses performed on TIM-1 gastric and ileal effluents have shown that the expression of major EHEC O157:H7 bacterial virulence genes was significantly higher under child digestive conditions, compared to the adult ones (12). Regarding *C. parvum*, although differences in digestive physicochemical properties between infants and adults may influence the amount, physiological state

457 and invasiveness of sporozoites released in the small intestine, they may not be associated with
458 significant modulation of parasite genes associated with virulence.

459 Transcriptomic analysis performed on TIM-1 gastric effluents collected within the initial twenty
460 minutes of digestion detected a low number of DEGs between stomach and inoculum samples,
461 predominantly exhibiting upregulation. In this digestive compartment, where most parasites were
462 found as intact oocysts, enrichment of upregulated genes associated with gene expression and
463 translation was detected. Similarly, previous transcriptomic analysis has revealed that the *C. parvum*
464 oocyst stage is highly active in protein synthesis, as evidenced by high transcripts levels of parasite
465 genes involved in ribosome biogenesis, transcription and translation (49).

466 We also analysed the *C. parvum* transcriptome collected from TIM-1 ileal effluents between 120 and
467 180 min of digestion, when the vast majority of parasites are found as released sporozoites compared
468 to the stomach compartment. Our RNA-Seq analysis revealed that the sporozoite-enriched
469 transcriptome exhibited much greater modulation in the ileum compared to the stomach, with
470 approximately 25% of upregulated genes associated with gene expression, nucleus or intracellular
471 structures and organelles. KEGG analysis highlighted the glycolysis/gluconeogenesis as a significantly
472 downregulated pathway in parasites collected from ileal effluents. Although *C. parvum* may possess a
473 remnant mitochondrion, it lacks the Krebs cycle and the cytochrome-based respiration, therefore
474 relying mainly, if not only, on glycolysis for ATP production (50). Glycolysis-related genes are known
475 to be highly expressed in intracellular developmental stages (51), supporting *C. parvum* replication
476 inside host cells. While some of their related products have also been detected in the sporozoite
477 proteome (52), they were found under-represented in this repertoire in another proteomic study (53).

478 Previous transcriptomic analysis has shown that, in contrast to intracellular developmental stages, *C.*
479 *parvum* extracellular stages (*i.e.*, oocysts and sporozoites) express a wider range of genes encoding
480 specialised functions (54), with few identified orthologs outside or related protozoan organisms. Like
481 other apicomplexan parasites, the polarised *C. parvum* sporozoites harbour unique apical secretory
482 organelles involved in attachment, invasion, penetration and maintenance of the parasite within the
483 host cell, (*i.e.*, micronemes, dense granules, small granules and a single rhoptry), as well as the

484 canonical glideosome dependent on actin and myosin providing parasite gliding motility (55–57).
485 Accordingly, the expression of several parasite genes associated with the latter apicomplexan feature,
486 particularly the myosin complex and cytoskeletal motor activity, was significantly modulated in the
487 sporozoite-enriched fractions collected from the TIM-1 ileal effluents. While two of these genes (Gene
488 IDs CPATCC_0009620 and CPATCC_0025920) showed a moderate downregulation in these
489 samples, two other encoding a protein from the actin family (Gene ID CPATCC_0036850) and a
490 myosin motor domain containing protein (Gene ID CPATCC_0021030) were characterised by a
491 tremendous 40- or ~ 2000-fold upregulation, respectively. Alongside this marked regulation of genes
492 potentially related to parasite gliding motility, the expression of genes encoding putative secreted
493 proteins was significantly modulated in ileal effluents. For instance, the expression levels of the
494 mucin-like glycoprotein GP900 (Gene ID CPATCC_0009860) were significantly downregulated in
495 our ileal sporozoite-enriched samples. Stored in the sporozoite micronemes and previously
496 hypothesised to be involved in attachment and/or invasion (58), the immunodominant protein GP900
497 has recently been shown to enter the secretory pathway after excystation, where its short cytoplasmic
498 domain is cleaved before discharge of the cleaved form to the extracellular space, suggesting a
499 lubrication role during sporozoite invasion (59). Finally, six genes encoding putative secreted proteins
500 were significantly upregulated in the TIM-1 ileal effluents, consistent with the past detection of
501 several proteins associated with extracellular protein secretion in the protein repertoire of *C. parvum*
502 sporozoites (52,53). Apart from a predicted hydrolase, the function of these putative secreted proteins
503 is not yet known. Interestingly, three of these genes are predicted to encode proteins belonging to the
504 SKSR family (Gene IDs CPATCC_0030860, CPATCC_0000030 and CPATCC_0035410). This
505 *Cryptosporidium*-specific multigene family comprises most highly polymorphic and subtelomeric
506 genes encoding secreted proteins harbouring a signal peptide and SK and SR repeats (60). Although
507 present in all major human-infecting *Cryptosporidium* species, differences in the presence or absence,
508 as well as in the copy numbers of this subtelomeric gene family, were recently identified between
509 sequenced *Cryptosporidium* genomes by comparative genomic analyses, similarly to two other
510 families encoding the MEDLE secretory proteins, named after their conserved sequence motif at the
511 C-terminus, and insulinase-like proteases (61–66). Recent findings identified SKSR1 as a member of

the secretory proteins (67) in the newly identified small granules organelles (57). Additionally, SKSR1 was shown to be secreted into the parasite-host interface (*i.e.*, parasitophorous vacuole membrane and feeder organelle) and to be important for *C. parvum* pathogenicity, suggesting that it may act as a virulence factor through regulating host responses (67). More comparative studies are needed to fully elucidate the function of all SKSR members, since gene gains and losses of this subtelomeric gene family are suggested to contribute to differences in pathogenicity and host specificity in *Cryptosporidium* populations.

CONCLUSIONS

Being one of the most common causes of infectious moderate-to-severe diarrhoea in young children, cryptosporidiosis is an important contributor to early childhood mortality in low-resource settings. Increased susceptibility of infants and toddlers to *Cryptosporidium* can be attributed to immature immune status in this age group. Using the sophisticated TIM-1 *in vitro* gastrointestinal model, we showed that the digestive physicochemical parameters encountered in the child digestive tract could be associated with fewer, however potentially more active and invasive sporozoites released. Our results suggest that age-mediated variation in the human gastrointestinal physiology could also partially explain why young individuals are more at risk. The link between specificities of the child digestive tract and disease is complex. Understanding the interactions between *C. parvum* infection and various digestive components of young individuals, including physicochemical parameters, mucus barrier, and microbiota, can provide us with a more accurate picture of children susceptibility, and possible valuable information towards new treatment strategies.

LIST OF ABBREVIATIONS

ATP: Adenosine triphosphate

C. andersoni: *Cryptosporidium andersoni*

C. hominis: *Cryptosporidium hominis*

536 *C. muris*: *Cryptosporidium muris*

537 *C. parvum*: *Cryptosporidium parvum*

538 DEG: Differentially expressed gene

539 DNA: Deoxyribonucleic acid

540 DNase: Deoxyribonuclease

541 *E. coli*: *Escherichia coli*

542 EHEC O157:H7: Enterohemorrhagic *Escherichia coli* serotype O157:H7

543 FBS: Fetal bovine serum

544 FDR: False discovery rate

545 GO: Gene ontology

546 GP900: Glycoprotein-900

547 IFN-γ: Interferon gamma

548 KEGG: Kyoto encyclopedia of genes and genomes

549 KO: Knock-out

550 Nluc: Nanoluciferase

551 PBS: Phosphate-buffered saline

552 PCA: Principal component analysis

553 RLU: Relative light unit

554 RNA: Ribonucleic acid

555 RNA-Seq: RNA sequencing

556 RPMI: Roswell Park Memorial Institute

557 SEM: Standard error of the mean

558 TIM-1: TNO (Toegepast Natuurwetenschappelijk Onderzoek) gastrointestinal model-1

DECLARATIONS

Ethics approval and consent to participate

Not applicable

Consent for publication

Not applicable

Availability of data and materials

The datasets generated and analysed during the current study are available in the GEO repository database, under accession number GSE271211 (https://www.ncbi.nlm.nih.gov/geo/query/acc.cgi?&acc=GSE271211).

Competing interests

The authors declare that they have no competing interests.

Funding

This research was supported by the INRAE Animal Health division and by the Laboratoire d'Excellence (LabEx) ParaFrap (ANR-11-LABX- 0024).

Author's contributions

JT, LE-M, SB-D and SL-L designed the project and the experiments. JT, LE-M, SC, AS, SD, CM and SL-L performed the experiments. JT and AS produced and purified the oocysts of the *C. parvum* INRAE Nluc strain. LE-M, SC, SD and CM performed the *in vitro* digestions. SL-L performed the flow cytometry analysis with the help of CB. JT performed the sporozoite luciferase activity and the cell culture experiments. AS performed the parasite RNA extractions. JT and GS analysed the RNA-Seq data. JT, LE-M, GS, FL, SB-D and SL-L interpreted the experimental work. JT, LE-M, FL, SB-D

and SL-L secured funding. JT, LE-M, SB-D and SL-L wrote the paper with editorial support and comments from all other authors. All authors read and approved the final version of the manuscript.

Acknowledgments

We would like to thank the Helixio company for the mRNA sequencing and bioinformatics analysis. We are also very grateful to Elise Courtot (UMR ISP, INRAE) for her help on statistical analysis.

REFERENCES

1. Checkley W, White AC, Jaganath D, Arrowood MJ, Chalmers RM, Chen XM, et al. A review of the global burden, novel diagnostics, therapeutics, and vaccine targets for Cryptosporidium. Lancet Infect Dis. 2015;15(1):85–94.

2. Kotloff KL, Nataro JP, Blackwelder WC, Nasrin D, Farag TH, Panchalingam S, et al. Burden and aetiology of diarrhoeal disease in infants and young children in developing countries (the Global Enteric Multicenter Study, GEMS): a prospective, case-control study. Lancet. 2013;382(9888):209–22.

3. Platts-Mills JA, Babji S, Bodhidatta L, Gratz J, Haque R, Havt A, et al. Pathogen-specific burdens of community diarrhoea in developing countries: a multisite birth cohort study (MAL-ED). Lancet Glob Health. 2015;3(9):e564-575.

4. Mølbak K, Højlyng N, Gottschau A, Sá JC, Ingholt L, da Silva AP, et al. Cryptosporidiosis in infancy and childhood mortality in Guinea Bissau, west Africa. BMJ. 1993;307(6901):417–20.

5. Khalil IA, Troeger C, Rao PC, Blacker BF, Brown A, Brewer TG, et al. Morbidity, mortality, and long-term consequences associated with diarrhoea from Cryptosporidium infection in children younger than 5 years: a meta-analyses study. Lancet Glob Health. 2018;6(7):e758–68.

6. Shirley DAT, Moonah SN, Kotloff KL. Burden of disease from cryptosporidiosis. Curr Opin Infect Dis. 2012;25(5):555–63.

7. English ED, Guérin A, Tandel J, Striepen B. Live imaging of the Cryptosporidium parvum life cycle reveals direct development of male and female gametes from type I meronts. PLoS Biol. 2022;20(4):e3001604.

8. Laurent F, Lacroix-Lamandé S. Innate immune responses play a key role in controlling infection of the intestinal epithelium by Cryptosporidium. Int J Parasitol. 2017;47(12):711–21.

9. Kaye JL. Review of paediatric gastrointestinal physiology data relevant to oral drug delivery. Int J Clin Pharm. 2011;33(1):20–4.

10. Uriot O, Chalancon S, Mazal C, Etienne-Mesmin L, Denis S, Blanquet-Diot S. Use of the dynamic TIM-1 model for an in-depth understanding of the survival and virulence gene expression of Shiga toxin-producing Escherichia coli in the human stomach and small intestine. Methods Mol Biol. 2021;2291:297–315.

11. Miszczycha SD, Thévenot J, Denis S, Callon C, Livrelli V, Alric M, et al. Survival of Escherichia coli O26:H11 exceeds that of Escherichia coli O157:H7 as assessed by simulated human digestion of contaminated raw milk cheeses. Int J Food Microbiol. 2014;172:40–8.

12. Roussel C, Cordonnier C, Galia W, Le Goff O, Thévenot J, Chalancon S, et al. Increased EHEC survival and virulence gene expression indicate an enhanced pathogenicity upon simulated pediatric gastrointestinal conditions. Pediatr Res. 2016;80(5):734–43.

13. Roussel C, De Paepe K, Galia W, De Bodt J, Chalancon S, Leriche F, et al. Spatial and temporal modulation of enterotoxigenic E. coli H10407 pathogenesis and interplay with microbiota in human gut models. BMC Biol. 2020;18(1):141.

14. Roussel C, De Paepe K, Galia W, de Bodt J, Chalancon S, Denis S, et al. Multi-targeted properties of the probiotic Saccharomyces cerevisiae CNCM I-3856 against enterotoxigenic Escherichia coli (ETEC) H10407 pathogenesis across human gut models. Gut Microbes. 2021;13(1):1953246.

15. Cavestri C, Savard P, Fliss I, Emond-Rhéault JG, Hamel J, Kukavica-Ibrulj I, et al. Salmonella enterica subsp. enterica virulence potential can be linked to higher survival within a dynamic in vitro human gastrointestinal model. Food Microbiol. 2022;101:103877.

16. Sauvaitre T, Van Landuyt J, Durif C, Roussel C, Sivignon A, Chalancon S, et al. Role of mucus-bacteria interactions in Enterotoxigenic Escherichia coli (ETEC) H10407 virulence and interplay with human microbiome. NPJ Biofilms Microbiomes. 2022;8(1):86.

17. Swale C, Bougdour A, Gnahoui-David A, Tottey J, Georgeault S, Laurent F, et al. Metal-captured inhibition of pre-mRNA processing activity by CPSF3 controls Cryptosporidium infection. Sci Transl Med. 2019;11(517):eaax7161.

18. Dobin A, Davis CA, Schlesinger F, Drenkow J, Zaleski C, Jha S, et al. STAR: ultrafast universal RNA-seq aligner. Bioinformatics. 2013;29(1):15–21.

19. Love MI, Huber W, Anders S. Moderated estimation of fold change and dispersion for RNA-seq data with DESeq2. Genome Biol. 2014;15(12):550.

20. Robinson MD, McCarthy DJ, Smyth GK. edgeR: a Bioconductor package for differential expression analysis of digital gene expression data. Bioinformatics. 2010;26(1):139–40.

21. Ashburner M, Ball CA, Blake JA, Botstein D, Butler H, Cherry JM, et al. Gene ontology: tool for the unification of biology. The Gene Ontology Consortium. Nat Genet. 2000;25(1):25–9.

22. Gene Ontology Consortium, Aleksander SA, Balhoff J, Carbon S, Cherry JM, Drabkin HJ, et al. The Gene Ontology knowledgebase in 2023. Genetics. 2023;224(1):iyad031.

23. Kanehisa M, Goto S. KEGG: kyoto encyclopedia of genes and genomes. Nucleic Acids Res. 2000;28(1):27–30.

24. Kanehisa M. Toward understanding the origin and evolution of cellular organisms. Protein Sci. 2019;28(11):1947–51.

25. Kanehisa M, Furumichi M, Sato Y, Kawashima M, Ishiguro-Watanabe M. KEGG for taxonomy-based analysis of pathways and genomes. Nucleic Acids Research. 2023;51(1):587-D592.

26. Heiges M, Wang H, Robinson E, Aurrecoechea C, Gao X, Kaluskar N, et al. CryptoDB: a Cryptosporidium bioinformatics resource update. Nucleic Acids Res. 2006;34:419–22.

27. Noguchi K, Gel YR, Brunner E, Konietschke F. nparLD: An R Software Package for the Nonparametric Analysis of Longitudinal Data in Factorial Experiments. Journal of Statistical Software. 2012;50:1–23.

28. Konietschke F, Placzek M, Schaarschmidt F, Hothorn LA. nparcomp: An R Software Package for Nonparametric Multiple Comparisons and Simultaneous Confidence Intervals. Journal of Statistical Software. 2015;64:1–17.

29. Smith HV, Nichols RAB, Grimason AM. Cryptosporidium excystation and invasion: getting to the guts of the matter. Trends Parasitol. 2005;21(3):133–42.

30. Widmer G, Klein P, Bonilla R. Adaptation of Cryptosporidium oocysts to different excystation conditions. Parasitology. 2007;134(11):1583–8.

31. Robertson LJ, Campbell AT, Smith HV. In vitro excystation of Cryptosporidium parvum. Parasitology. 1993;106:13–9.

32. Forney JR, Yang S, Healey MC. Protease activity associated with excystation of Cryptosporidium parvum oocysts. J Parasitol. 1996;82(6):889–92.

33. Okhuysen PC, Chappell CL, Kettner C, Sterling CR. Cryptosporidium parvum metalloaminopeptidase inhibitors prevent in vitro excystation. Antimicrob Agents Chemother. 1996;40(12):2781–4.

34. King BJ, Keegan AR, Phillips R, Fanok S, Monis PT. Dissection of the hierarchy and synergism of the bile derived signal on Cryptosporidium parvum excystation and infectivity. Parasitology. 2012;139(12):1533–46.

35. Omari TI, Davidson GP. Multipoint measurement of intragastric pH in healthy preterm infants. Arch Dis Child Fetal Neonatal Ed. 2003;88(6):517–20.

36. Koziolek M, Grimm M, Becker D, Iordanov V, Zou H, Shimizu J, et al. Investigation of pH and Temperature Profiles in the GI Tract of Fasted Human Subjects Using the Intellicap(®) System. J Pharm Sci. 2015;104(9):2855–63.

37. Challacombe DN, Edkins S, Brown GA. Duodenal bile acids in infancy. Arch Dis Child. 1975;50(11):837–43.

38. Vertzoni M, Archontaki H, Reppas C. Determination of intralumenal individual bile acids by HPLC with charged aerosol detection. J Lipid Res. 2008;49(12):2690–5.

39. Vítovec J, Koudela B. Pathogenesis of intestinal cryptosporidiosis in conventional and gnotobiotic piglets. Vet Parasitol. 1992;43(1–2):25–36.

40. Kelly P, Makumbi FA, Carnaby S, Simjee AE, Farthing MJG. Variable distribution of Cryptosporidium parvum in the intestine of AIDS patients revealed by polymerase chain reaction. Eur J Gastroenterol Hepatol. 1998;10(10):855.

41. Current WL, Garcia LS. Cryptosporidiosis. Clin Microbiol Rev. 1991;4(3):325–58.

42. de Graaf DC, Vanopdenbosch E, Ortega-Mora LM, Abbassi H, Peeters JE. A review of the importance of cryptosporidiosis in farm animals. Int J Parasitol. 1999;29(8):1269–87.

43. Gallego-Lopez GM, Mendoza Cavazos C, Tibabuzo Perdomo AM, Garfoot AL, O'Connor RM, Knoll LJ. Dual transcriptomics to determine gamma interferon-independent host response to intestinal Cryptosporidium parvum infection. Infect Immun. 2022;90(2):e0063821.

693 44. Delachaume-Salem E, Sarles H. [Normal human pancreatic secretion in relation to age]. Biol
694 Gastroenterol (Paris). 1970;2:135□46.

695 45. Kalantzi L, Goumas K, Kalioras V, Abrahamsson B, Dressman JB, Reppas C. Characterization of
696 the human upper gastrointestinal contents under conditions simulating
697 bioavailability/bioequivalence studies. Pharm Res. 2006;23(1):165□76.

698 46. Arrowood MJ. In vitro cultivation of cryptosporidium species. Clin Microbiol Rev.
699 2002;15(3):390□400.

700 47. Matsubayashi M, Ando H, Kimata I, Nakagawa H, Furuya M, Tani H, et al. Morphological
701 changes and viability of Cryptosporidium parvum sporozoites after excystation in cell-free culture
702 media. Parasitology. 2010;137(13):1861□6.

703 48. Castellanos-Gonzalez A, Perry N, Nava S, White AC. Preassembled single-stranded RNA-
704 Argonaute complexes: a novel method to silence genes in Cryptosporidium. J Infect Dis.
705 2016;213(8):1307□14.

706 49. Zhang H, Guo F, Zhou H, Zhu G. Transcriptome analysis reveals unique metabolic features in the
707 Cryptosporidium parvum Oocysts associated with environmental survival and stresses. BMC
708 Genomics. 2012;13:647.

709 50. Abrahamsen MS, Templeton TJ, Enomoto S, Abrahante JE, Zhu G, Lancto CA, et al. Complete
710 genome sequence of the apicomplexan, Cryptosporidium parvum. Science. 2004;304(5669):441□5.

711 51. Mauzy MJ, Enomoto S, Lancto CA, Abrahamsen MS, Rutherford MS. The Cryptosporidium
712 parvum transcriptome during in vitro development. PLoS One. 2012;7(3):e31715.

713 52. Snelling WJ, Lin Q, Moore JE, Millar BC, Tosini F, Pozio E, et al. Proteomics analysis and protein
714 expression during sporozoite excystation of Cryptosporidium parvum (Coccidia, Apicomplexa).
715 Mol Cell Proteomics. 2007;6(2):346□55.

716 53. Sanderson SJ, Xia D, Prieto H, Yates J, Heiges M, Kissinger JC, et al. Determining the protein
717 repertoire of Cryptosporidium parvum sporozoites. Proteomics. 2008;8(7):1398□414.

718 54. Matos LVS, McEvoy J, Tzipori S, Bresciani KDS, Widmer G. The transcriptome of
719 Cryptosporidium oocysts and intracellular stages. Sci Rep. 2019;9(1):7856.

720 55. Wetzel DM, Schmidt J, Kuhlenschmidt MS, Dubey JP, Sibley LD. Gliding motility leads to active
721 cellular invasion by Cryptosporidium parvum sporozoites. Infect Immun. 2005;73(9):5379□87.

722 56. Guérin A, Striepen B. The biology of the intestinal intracellular parasite Cryptosporidium. Cell
723 Host Microbe. 2020;28(4):509□15.

724 57. Guérin A, Strelau KM, Barylyuk K, Wallbank BA, Berry L, Crook OM, et al. *Cryptosporidium*
725 uses multiple distinct secretory organelles to interact with and modify its host cell. Cell Host
726 Microbe. 2023;31(4):650-664.e6.

727 58. Barnes DA, Bonnin A, Huang JX, Gousset L, Wu J, Gut J, et al. A novel multi-domain mucin-like
728 glycoprotein of *Cryptosporidium parvum* mediates invasion. Mol Biochem Parasitol.
729 1998;96(1):93□110.

730 59. Li X, Yin J, Wang D, Gao X, Zhang Y, Wu M, et al. The mucin-like, secretory type-I
731 transmembrane glycoprotein GP900 in the apicomplexan Cryptosporidium parvum is cleaved in the
732 secretory pathway and likely plays a lubrication role. Parasit Vectors. 2022;15(1):170.

60. Widmer G, Carmena D, Kváč M, Chalmers RM, Kissinger JC, Xiao L, et al. Update on Cryptosporidium spp.: highlights from the Seventh International Giardia and Cryptosporidium Conference. Parasite. 2020;27:14.

61. Guo Y, Tang K, Rowe LA, Li N, Roellig DM, Knipe K, et al. Comparative genomic analysis reveals occurrence of genetic recombination in virulent Cryptosporidium hominis subtypes and telomeric gene duplications in Cryptosporidium parvum. BMC Genomics. 2015;16(1):320.

62. Isaza JP, Galván AL, Polanco V, Huang B, Matveyev AV, Serrano MG, et al. Revisiting the reference genomes of human pathogenic Cryptosporidium species: reannotation of C. parvum Iowa and a new C. hominis reference. Sci Rep. 2015;5:16324.

63. Feng Y, Li N, Roellig DM, Kelley A, Liu G, Amer S, et al. Comparative genomic analysis of the IId subtype family of Cryptosporidium parvum. Int J Parasitol. 2017;47(5):281□90.

64. Xu Z, Li N, Guo Y, Feng Y, Xiao L. Comparative genomic analysis of three intestinal species reveals reductions in secreted pathogenesis determinants in bovine-specific and non-pathogenic Cryptosporidium species. Microb Genom. 2020;6(6):e000379.

65. Wang T, Guo Y, Roellig DM, Li N, Santín M, Lombard J, et al. Sympatric recombination in zoonotic Cryptosporidium leads to emergence of populations with modified host preference. Mol Biol Evol. 2022;39(7):msac150.

66. Li J, Li N, Roellig DM, Zhao W, Guo Y, Feng Y, et al. High subtelomeric GC content in the genome of a zoonotic Cryptosporidium species. Microb Genom. 2023;9(7):mgen001052.

67. He W, Sun L, Hou T, Yang Z, Yang F, Wang T, et al. SKSR1 identified as key virulence factor in Cryptosporidium by genetic crossing. BioRxiv. 2024;(577707).

FIGURE 1

Title. TIM-1 experimental set-up and analysis.

Legend. The left side shows a picture of the TIM-1 system composed of four successive compartments simulating the human stomach and the three parts of the small intestine (*i.e.*, the duodenum, jejunum and ileum) mimicking the main physicochemical parameters of human gastrointestinal digestion. Digestion experiments were performed to reproduce an adult or an infant (from 6 months old to 2 years old) ingesting a glass of water contaminated with 1×10^8 oocysts of the *C. parvum* INRAE Nluc strain. On the right side, sampling times (minutes) are indicated when samples were taken either directly from each compartment (for flow cytometry, sporozoite luciferase activity and invasion assay); or indirectly by pooling the gastric effluents when the stomach compartment was solely used, or the ileal effluents when the entire TIM-1 system was used (for RNA

766 sequencing). Digestions were run in triplicate. Created with BioRender.com (Agreement number:
767 JH26ZFM4TU).

768 FIGURE 2

769 **Title.** *Cryptosporidium parvum* excystation in the human *in vitro* upper gastrointestinal tract.

770 **Legend. (A)** Flow cytometry gating strategy on forward-angle light scatter/side-angle light scatter
771 established during *in vitro* excystation of parasites, allowing detection of intact oocysts, empty oocyst
772 shells and sporozoites. Created with BioRender.com (Agreement number: FF26ZFMVSM). **(B)**
773 Parasite excystation during child or adult digestion in the TIM-1 system. Cytograms obtained for one
774 representative experiment for the child or the adult digestion at 45 min in the stomach and at 60 min in
775 the duodenum show the timing when excystation occurs in the *in vitro* gastrointestinal tract.

776 FIGURE 3

777 **Title.** Physiological state and invasion ability of *Cryptosporidium parvum* sporozoites collected from
778 the TIM-1 system.

779 **Legend. (A)** Luciferase activity expressed by *C. parvum* sporozoites collected from the duodenal
780 (Duo), jejunal (Jej) or ileal (Ile) TIM-1 compartments during child (purple) or adult (dark blue)
781 digestion. Boxplots depict the relative luminescence of sporozoites compared with that of the
782 inoculum for each digestion assay. For each age condition, significant differences ($P < 0.05$) between
783 time points are indicated by non-corresponding letters (purple lowercase for child digestion and blue
784 capitals for adult digestion). For each time point, significant differences between age conditions are
785 indicated in black as follows: **** $P < 0.0001$. **(B)** Invasion assay. *C. parvum* sporozoites were
786 allowed to infect HCT-8 monolayers for 2.5 h before evaluation of luminescence intensity. Boxplots
787 depict the luminescence measured in infected cells from which the luciferase background measured in
788 non-infected cells has been removed. For each age condition, significant differences ($P < 0.01$ or $P <$
789 0.001 for child or adult, respectively) between time points are indicated by non-corresponding letters

(purple lowercase for child digestion and blue capitals for adult digestion). For each time point, significant differences between age conditions are indicated in black as follows: ** $P < 0.01$.

FIGURE 4

Title. RNA-Seq analysis of *C. parvum* genes in TIM-1 samples.

Legend. **(A)** Principal component analysis of RNA-Seq samples investigating gene expression changes in *C. parvum* parasites collected in the inoculum (t = 0 min), or in gastric (0-20 min) or ileal effluents (120-180 min) during the simulated child or adult digestions in the TIM-1. PCA was performed using normalised RNA-Seq data of a set of 2430 filtered genes. **(B)** Number of differentially expressed genes (DEGs) between pairwise comparisons. All DEGs show an adjusted *P*-value < 0.05 and a minimal regulation of 2-fold (log2FC > 1). **(C)** Number of upregulated (green) or downregulated (orange) genes between samples collected from different TIM-1 compartments in both child and adult conditions. The number of DEGs shared by age conditions is shown in brackets and with the dotted filling pattern.

FIGURE 5

Title. Enrichment analysis on *C. parvum* genes differentially expressed in the ileal compartment.

Legend. The Gene Ontology and KEGG enrichment analysis was performed on genes that were significantly up- or downregulated in the ileal effluents compared with the inoculum. The number of genes associated with each significantly enriched (*i.e.*, showing a Benjamini-Hochberg-adjusted *P*-value or FDR < 0.05) GO term or KEGG pathway is displayed for the child **(A)** or the adult **(B)** conditions. The three GO term categories named 'Biological process', 'Cellular component' and 'Molecular function' are represented by blue, green or orange bars, respectively. The KEGG Metabolic pathways are represented by grey bars. The GO terms or KEGG pathway shared by both age conditions are indicated by a star.

ADDITIONAL FILE 1

File format. Figure (.pdf)

Title of data. Luciferase activity expressed by live or heat-killed *C. parvum* INRAE Nluc parasites.

Description of data. Luciferase activity expressed by live or heat-killed *C. parvum* INRAE Nluc parasites. Luciferase activity was measured in live (*i.e.*, maintained at room temperature for 30 min, blue dots) or heat-killed (*i.e.*, maintained at 60°C for 30 min, red dots) *C. parvum* INRAE Nluc parasites, following excystation of 1×10^7 oocysts or 1×10^6 oocysts. Individual values from five independent experiments are represented. Significant differences between groups determined by Mann-Whitney non-parametric test are indicated as follows: ** $P < 0.01$. Cp, *Cryptosporidium parvum*. RT, room temperature.

ADDITIONAL FILE 2

File format. Excel spreadsheet (.xls)

Title of data. RNA-Seq Stomach Adult *vs* Stomach Child.

Description of data. Differentially expressed genes determined by RNA-sequencing between samples collected in gastric effluents of adult and gastric effluents of child, and results from enrichment analyses performed on significantly upregulated or downregulated genes.

ADDITIONAL FILE 3

File format. Excel spreadsheet (.xls)

Title of data. RNA-Seq Ileal Adult *vs* Ileal Child.

Description of data. Differentially expressed genes determined by RNA-sequencing between samples collected in ileal effluents of adult and ileal effluents of child, and results from enrichment analyses performed on significantly upregulated or downregulated genes.

ADDITIONAL FILE 4

File format. Excel spreadsheet (.xls)

Title of data. RNA-Seq Stomach Child *vs* Inoculum.

Description of data. Differentially expressed genes determined by RNA-sequencing between samples collected in gastric effluents of child and inoculum, and results from enrichment analyses performed on significantly upregulated or downregulated genes.

ADDITIONAL FILE 5

File format. Excel spreadsheet (.xls)

Title of data. RNA-Seq Stomach Adult *vs* Inoculum.

Description of data. Differentially expressed genes determined by RNA-sequencing between samples collected in gastric effluents of adult and inoculum, and results from enrichment analyses performed on significantly upregulated or downregulated genes.

ADDITIONAL FILE 6

File format. Figure (.pdf)

Title of data. Enrichment analysis on *C. parvum* genes differentially expressed in the stomach compared to the inoculum **(A)** or in the ileum compared to the stomach **(B)**.

Description of data. The Gene Ontology and KEGG enrichment analysis was performed on genes that were significantly up- or downregulated. The number of genes associated with each significantly enriched (*i.e.*, showing a Benjamini-Hochberg-adjusted *P*-value or FDR < 0.05) GO term or KEGG pathway is displayed for both child (left) and adult (right) conditions. The three GO term categories named 'Biological process', 'Cellular component' and 'Molecular function' are represented by blue, green or orange bars, respectively. The KEGG Metabolic pathways are represented by grey bars.

ADDITIONAL FILE 7

File format. Excel spreadsheet (.xls)

Title of data. RNA-Seq Ileal Child *vs* Stomach Child.

Description of data. Differentially expressed genes determined by RNA-sequencing between samples collected in ileal effluents of child and gastric effluents of child, and results from enrichment analyses performed on significantly upregulated or downregulated genes.

ADDITIONAL FILE 8

File format. Excel spreadsheet (.xls)

Title of data. RNA-Seq Ileal Adult *vs* Stomach Adult.

Description of data. Differentially expressed genes determined by RNA-sequencing between samples collected in ileal effluents of adult and gastric effluents of adult, and results from enrichment analyses performed on significantly upregulated or downregulated genes.

ADDITIONAL FILE 9

File format. Excel spreadsheet (.xls)

Title of data. RNA-Seq Ileal Child *vs* Inoculum.

Description of data. Differentially expressed genes determined by RNA-sequencing between samples collected in ileal effluents of child and inoculum, and results from enrichment analyses performed on significantly upregulated or downregulated genes.

ADDITIONAL FILE 10

File format. Excel spreadsheet (.xls)

877 **Title of data.** RNA-Seq Ileal Adult *vs* Inoculum.

878 **Description of data.** Differentially expressed genes determined by RNA-sequencing between samples
879 collected in ileal effluents of adult and inoculum, and results from enrichment analyses performed on
880 significantly upregulated or downregulated genes.

881

Figure 1

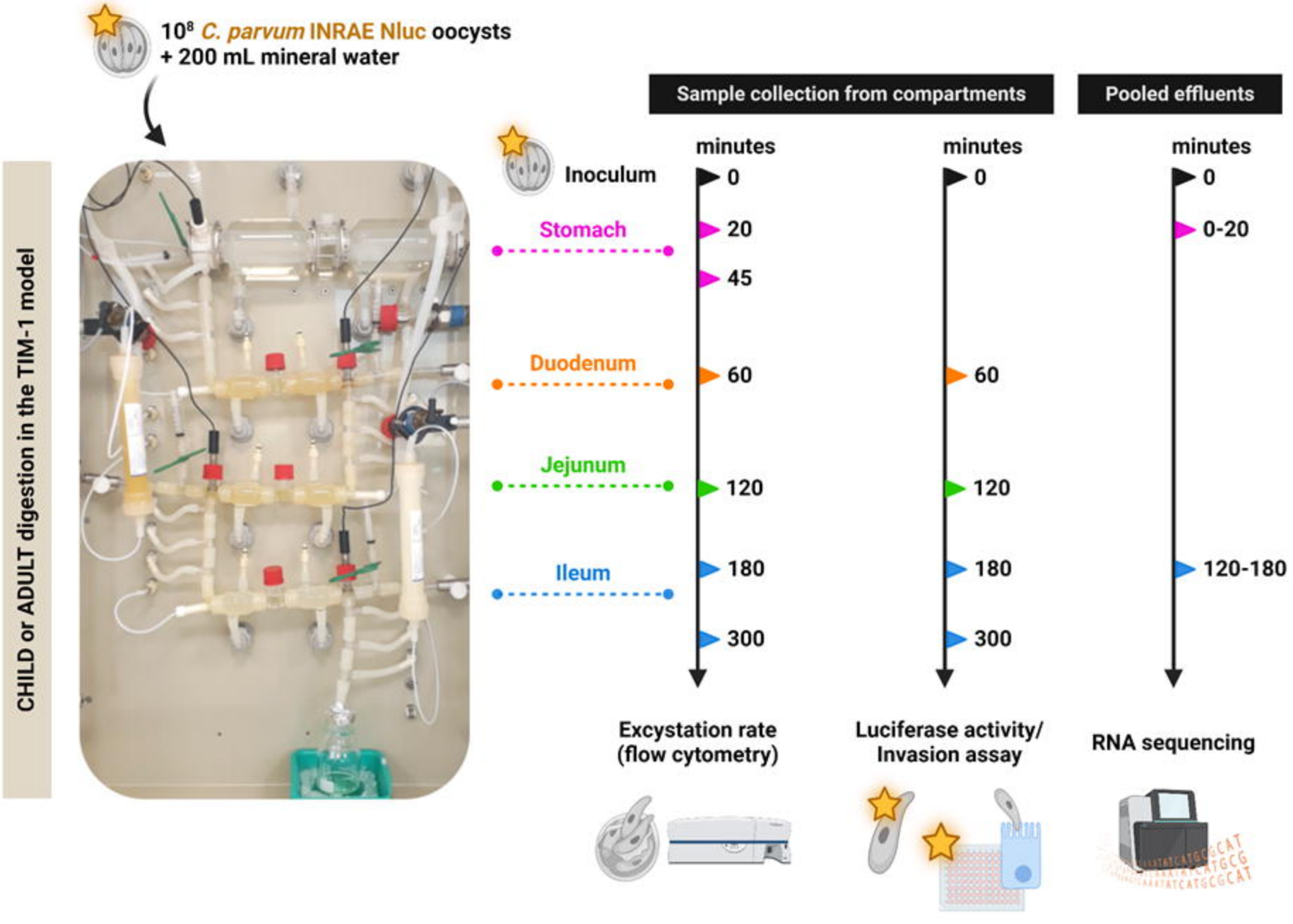
10^8 *C. parvum* INRAE Nluc oocysts
+ 200 mL mineral water
CHILD or ADULT digestion in the TIM-1 model
Sample collection from compartments
Pooled effluents
Inoculum
Stomach
Duodenum
Jejunum
Ileum
minutes
0
20
45
60
120
180
300
minutes
0
60
120
180
300
minutes
0
0-20
120-180
Excystation rate
(flow cytometry)
Luciferase activity/
Invasion assay
RNA sequencing

Figure 2

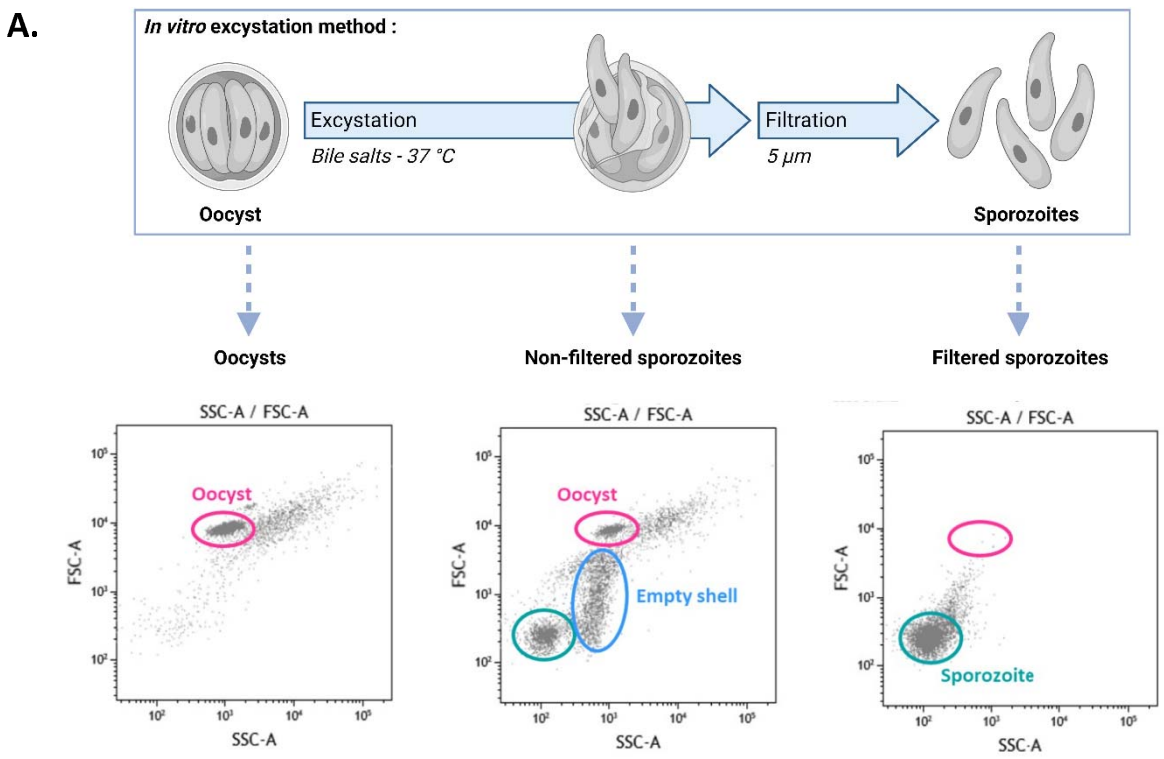

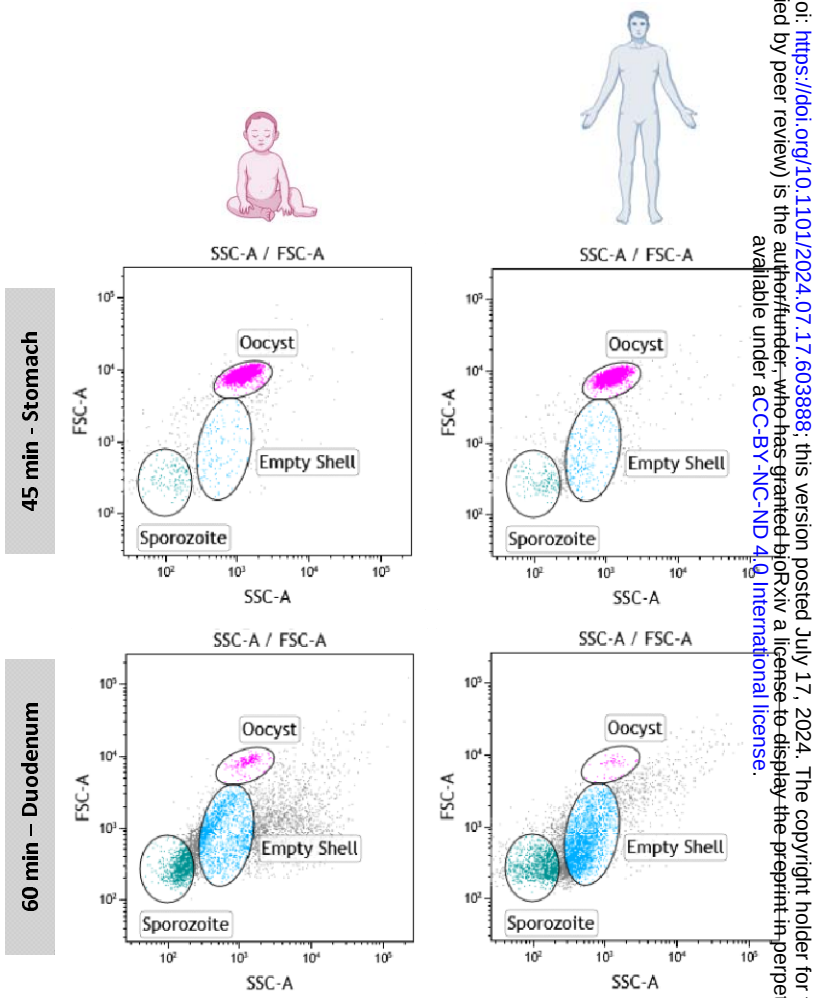

Figure 3

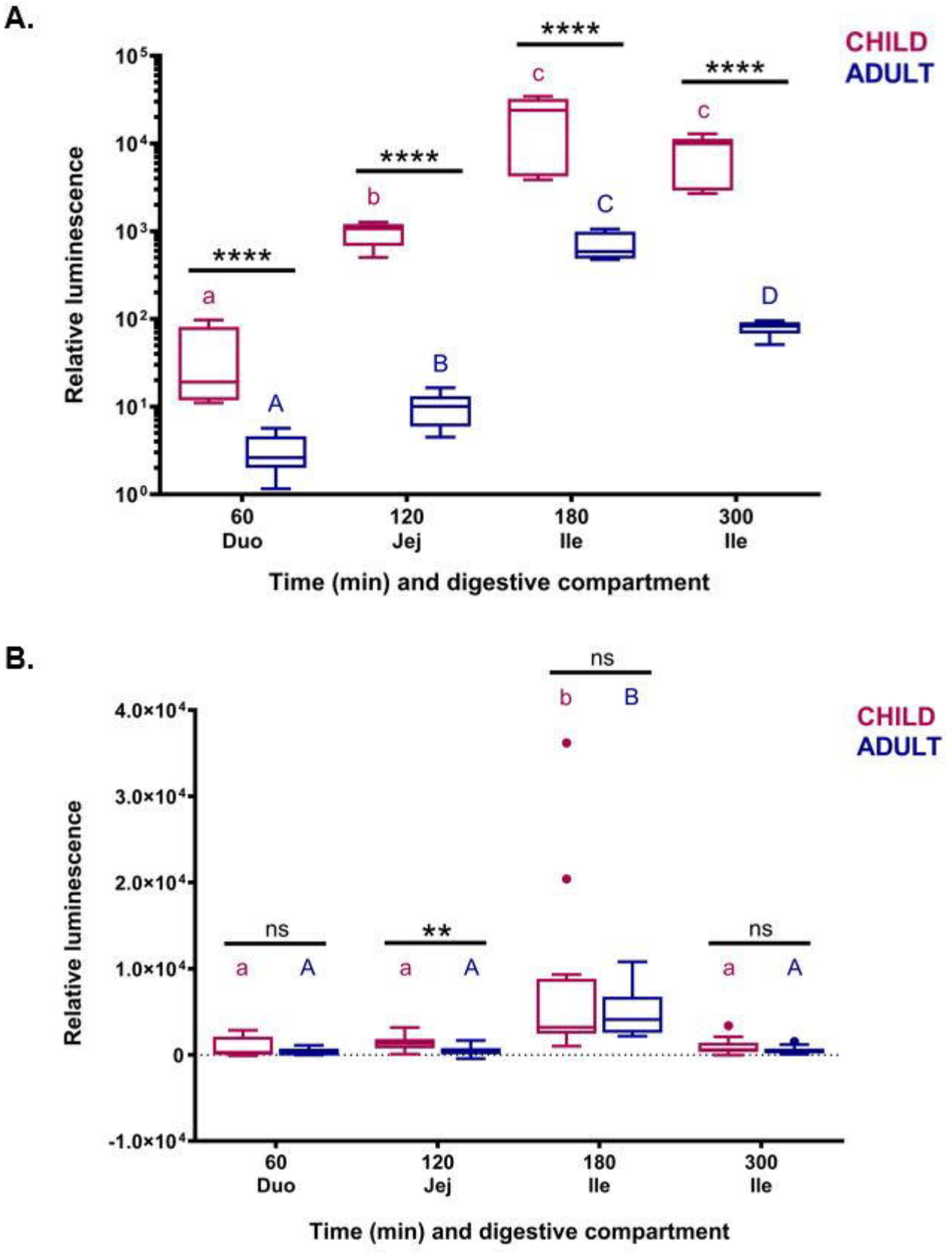
A.
CHILD
ADULT
Relative luminescence
10^5
10^4
10^3
10^2
10^1
10^0
****
****
****
a
A
b
B
c
C
c
D
60
Duo
120
Jej
180
Ile
300
Ile
Time (min) and digestive compartment
B.
CHILD
ADULT
Relative luminescence
4.0×10⁴
3.0×10⁴
2.0×10⁴
1.0×10⁴
0
-1.0×10⁴
ns
**
ns
ns
a
A
a
A
b
B
a
A
60
Duo
120
Jej
180
Ile
300
Ile
Time (min) and digestive compartment

Figure 4

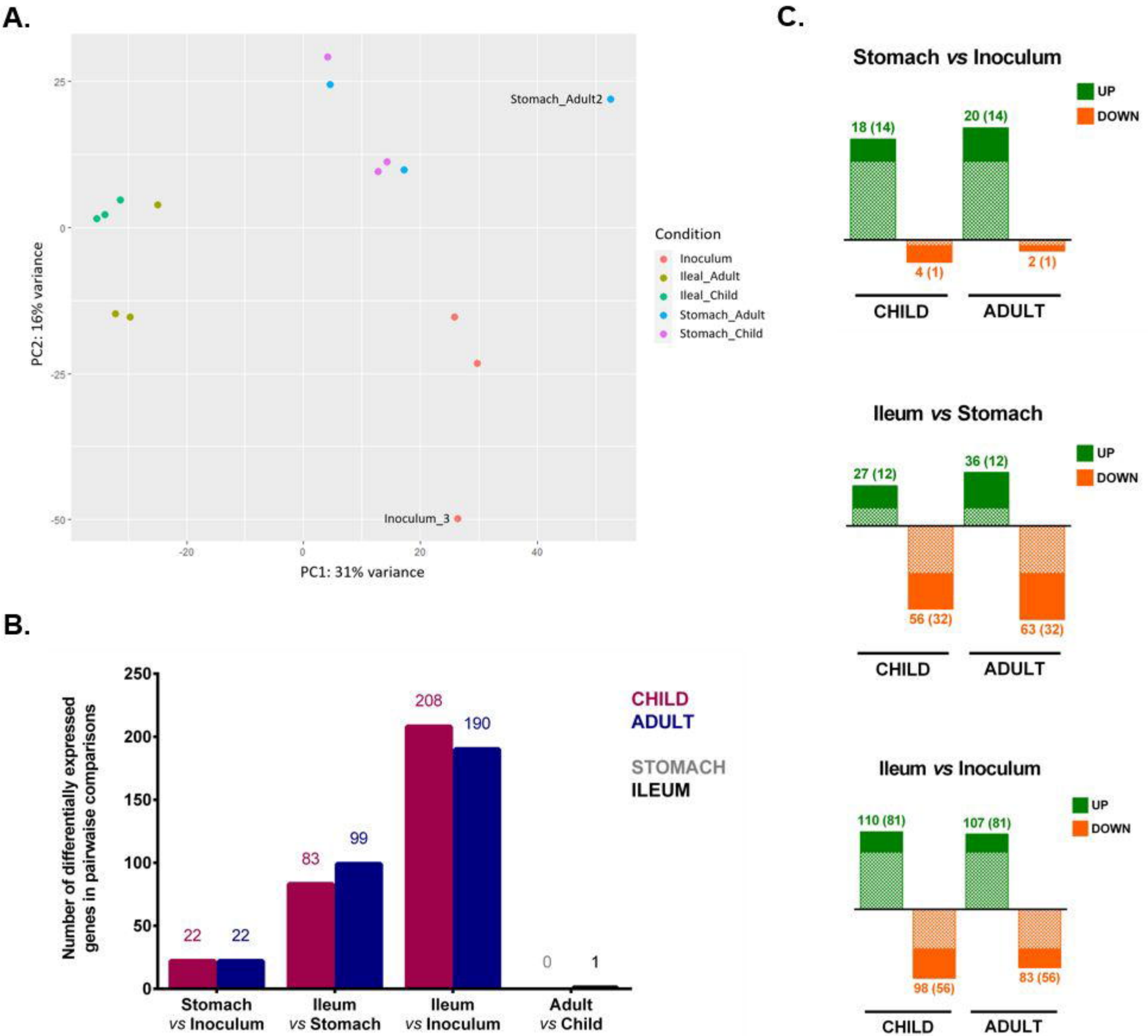
A.
Stomach_Adult2
Inoculum_3
PC2: 16% variance
PC1: 31% variance
Condition
Inoculum
Ileal_Adult
Ileal_Child
Stomach_Adult
Stomach_Child
B.
Number of differentially expressed genes in pairwaise comparisons
22
22
83
99
208
190
0
1
Stomach vs Inoculum
Ileum vs Stomach
Ileum vs Inoculum
Adult vs Child
CHILD
ADULT
STOMACH
ILEUM
C.
Stomach vs Inoculum
18 (14)
4 (1)
20 (14)
2 (1)
Ileum vs Stomach
27 (12)
56 (32)
36 (12)
63 (32)
Ileum vs Inoculum
110 (81)
98 (56)
107 (81)
83 (56)
UP
DOWN
CHILD
ADULT

Figure 5

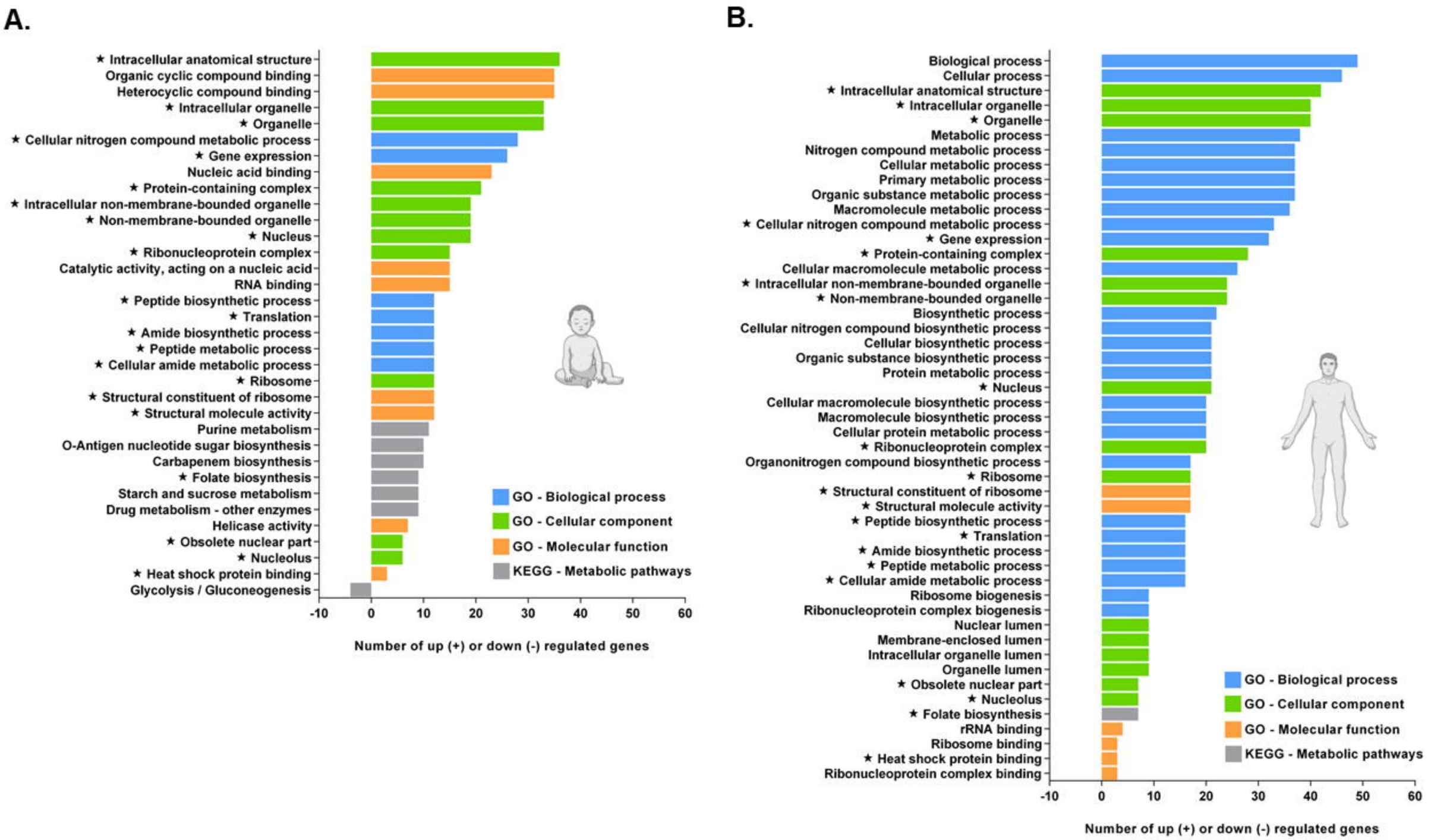
A.
★ Intracellular anatomical structure
Organic cyclic compound binding
Heterocyclic compound binding
★ Intracellular organelle
★ Organelle
★ Cellular nitrogen compound metabolic process
★ Gene expression
Nucleic acid binding
★ Protein-containing complex
★ Intracellular non-membrane-bounded organelle
★ Non-membrane-bounded organelle
★ Nucleus
★ Ribonucleoprotein complex
Catalytic activity, acting on a nucleic acid
RNA binding
★ Peptide biosynthetic process
★ Translation
★ Amide biosynthetic process
★ Peptide metabolic process
★ Cellular amide metabolic process
★ Ribosome
★ Structural constituent of ribosome
★ Structural molecule activity
Purine metabolism
O-Antigen nucleotide sugar biosynthesis
Carbapenem biosynthesis
★ Folate biosynthesis
Starch and sucrose metabolism
Drug metabolism - other enzymes
Helicase activity
★ Obsolete nuclear part
★ Nucleolus
★ Heat shock protein binding
Glycolysis / Gluconeogenesis
GO - Biological process
GO - Cellular component
GO - Molecular function
KEGG - Metabolic pathways
-10 0 10 20 30 40 50 60
Number of up (+) or down (-) regulated genes
B.
Biological process
Cellular process
★ Intracellular anatomical structure
★ Intracellular organelle
★ Organelle
Metabolic process
Nitrogen compound metabolic process
Cellular metabolic process
Primary metabolic process
Organic substance metabolic process
Macromolecule metabolic process
★ Cellular nitrogen compound metabolic process
★ Gene expression
★ Protein-containing complex
Cellular macromolecule metabolic process
★ Intracellular non-membrane-bounded organelle
★ Non-membrane-bounded organelle
Biosynthetic process
Cellular nitrogen compound biosynthetic process
Cellular biosynthetic process
Organic substance biosynthetic process
Protein metabolic process
★ Nucleus
Cellular macromolecule biosynthetic process
Macromolecule biosynthetic process
Cellular protein metabolic process
★ Ribonucleoprotein complex
Organonitrogen compound biosynthetic process
★ Ribosome
★ Structural constituent of ribosome
★ Structural molecule activity
★ Peptide biosynthetic process
★ Translation
★ Amide biosynthetic process
★ Peptide metabolic process
★ Cellular amide metabolic process
Ribosome biogenesis
Ribonucleoprotein complex biogenesis
Nuclear lumen
Membrane-enclosed lumen
Intracellular organelle lumen
Organelle lumen
★ Obsolete nuclear part
★ Nucleolus
★ Folate biosynthesis
rRNA binding
Ribosome binding
★ Heat shock protein binding
Ribonucleoprotein complex binding
GO - Biological process
GO - Cellular component
GO - Molecular function
KEGG - Metabolic pathways
-10 0 10 20 30 40 50 60
Number of up (+) or down (-) regulated genes